Acta Physiologiae Plantarum (2019) 41:167
https://doi.org/10.1007/s11738-019-2956-0

ORIGINAL ARTICLE

Chlorophyll *a* fluorescence analysis reveals divergent photosystem II responses to saline, alkaline and saline–alkaline stresses in the two *Lotus japonicus* model ecotypes MG20 and Gifu-129

César Daniel Bordenave[1] · Rubén Rocco[1] · Santiago Javier Maiale[1] · Maria Paula Campestre[1] · Oscar Adolfo Ruiz[1] · Andrés Alberto Rodríguez[1] · Ana Bernardina Menéndez[2]

Received: 24 September 2018 / Revised: 2 August 2019 / Accepted: 22 August 2019 / Published online: 31 August 2019

Abstract

Saline and alkaline stresses affect more than 10% of the World's arable land, limiting agricultural production. Salt-induced stress may affect the photosystem II (PSII) function, altering fluorescence emission. Therefore, changes in fluorescence are used to quantify and analyze abiotic stress responses in plants. So far, no study has focused on the response of PSII to saline, alkaline and saline–alkaline stresses in the model legume *Lotus japonicus*. For the saline, alkaline and saline–alkaline treatments, plants of the *L. japonicus* ecotypes MG20 and Gifu-129 were cultivated in sand with nutrient solution, added with NaCl and $NaHCO_3$ in different proportions. Growth, gas exchange, and chlorophyll *a* fluorescence transient kinetic and OJIP parameters were measured, and chlorophyll *a* and *b* were determined. The analysis of the kinetic of chlorophyll *a* fluorescence showed that NaCl-derived stress sources affect the photochemical events in PSII in both ecotypes, being this effect more evident under higher pH condition, whereas alkalinity per se has a mild or no effect on these events. The saline–alkaline stress induced a more severe effect on Gifu B-129, compared with Miyakojima MG20, whereas NaCl improved primary photochemistry in MG20. Our results allow us to accept the hypothesis that both ecotypes deploy differential responses under the three stressful treatments and that the saline–alkaline stress causes higher damage levels than saline and alkaline stresses alone in relation with structures and sub-processes of the PSII.

Keywords Alkalinity · Chlorophyll *a* fluorescence · *Lotus japonicus* · OJIP transient · Photosynthesis · Salinity

Communicated by U. Feller.

César Daniel Bordenave and Rubén Rocco should be regarded as first authors, both have contributed equally.

Electronic supplementary material The online version of this article (https://doi.org/10.1007/s11738-019-2956-0) contains supplementary material, which is available to authorized users.

✉ Ana Bernardina Menéndez
anamen@bg.fcen.uba.ar

César Daniel Bordenave
bordenavecesar@gmail.com

Rubén Rocco
rubenrocco04@gmail.com

Santiago Javier Maiale
smaiale@intech.gov.ar

Maria Paula Campestre
mpcampestre@intech.gov.ar

Oscar Adolfo Ruiz
ruiz@intech.gov.ar

Andrés Alberto Rodríguez
andres.a.rodriguez@gmail.com

[1] Instituto Tecnológico de Chascomús, Consejo Nacional de Investigaciones Científicas y Técnicas, Universidad Nacional de General San Martín (INTECH-CONICET-UNSAM), Intendente Marino KM 8.2-CC 164, B7130IWA Chascomús, Buenos Aires, Argentina

[2] Departamento de Biodiversidad y Biología Experimental, Facultad de Ciencias Exactas y Naturales, Instituto de Micología y Botánica (INMIBO-CONICET), Universidad de Buenos Aires, Piso 4 Pab II Ciudad Universitaria (1428), Buenos Aires, Argentina

Introduction

Saline stress represents a soil condition where neutral salts (NaCl or Na_2SO_4) predominate, whereas alkaline stress is mainly related to the occurrence of alkaline salts (Na_2CO_3 or $NaHCO_3$; Yang et al. 2007). Both salt stresses disturb more

than 10% of the world's cultivable area, hindering agricultural outputs (Läuchli and Lüttge 2002). Negative effects of saline stress include reduction of water uptake from soil (Munns 2002) and Na^+ or Cl^- build-up within cells, leading to enzymatic activity inhibition, all altering photosynthetic and energetic processes (Yeo 1998; Tester and Davenport 2003). Alkaline salts may cause deficiency of nutrients such as phosphorus, iron and zinc (Clark 1982; Clark et al. 1982; Marschner 1995), inhibiting photosynthesis and plant growth, besides altering balances of reactive oxygen species and causing cell dying (Kukavica et al. 2013). Fluctuating neutral to alkaline salt proportions often co-exist according to the soil (Shi and Wang 2005; Li et al. 2010). Several authors have reported that when mixed, saline and alkaline stresses present synergistic detrimental actions on plant development (e.g.: Shi and Sheng 2005; Paz et al. 2012, 2014; Vu et al. 2015; Li et al. 2017; Kumar et al. 2018; Jia et al. 2019).

Salt stress often limits the photosynthesis (Ashraf and Harris 2013). In the long term, salinity-induced reductions in the photosynthetic activity may result from decreases in the chlorophyll (Chl) and carotenoid contents (Parida and Das 2005; Munns and Tester 2008; Duarte et al. 2013), increased stomatal closure (Kyle et al. 1987) and/or non-stomatal restrictions, such as electron transport chain disruption (Parida and Das 2005; Chaves et al. 2009; Xiang et al. 2016), among other factors. Indeed, several stress sources may affect the photosystem II (PSII) function, which alters fluorescence emission. Therefore, changes in fluorescence are used to assess and analyze abiotic stress responses in plants (Demetriou et al. 2007; Kalaji et al. 2011; Mathur et al. 2013; Zushi and Matsuzoe 2017).

In plants, fluorescence is primarily produced by Chl *a* integrating the PSII antenna complexes. Its detection and analysis constitutes one of the most informative approaches to monitor the photosystem II (PSII) functioning. Changes in fluorescence are related to processes occurring within and around the PSII reaction centers, which reveal alterations in the acceptors redox balance and the energy quantum yield (Goltsev et al. 2016). After a dark-adapted plant has been illuminated, the intensity of Chl *a* fluorescence varies in a typical way. This variation in fluorescence intensity over time is acknowledged as fluorescence transient and may be represented by a polyphasic curve (or Kautsky curve, Papageorgiou 1975). This curve shows a phase of rapid increase presenting four steps symbolized as O–J–I–P (Strasser et al. 1995). The O–J–I–P test gives clues on the condition of quinone A (Q_A), quinone B (Q_B) and plastoquinone (PQ) pools (Strasser and Govindjee 1992). The rise of Chl *a* fluorescence from its minimal level "O" (the minimum value of fluorescence, F_0) to a "J" level (or F_J) occurs at about 2 ms as result of Q_A reduction by PSII; this is followed by a fluorescence rise to the "I" level (or F_I) at about 30 ms, by cause of the filling up of the quinone pool (Q_A and Q_B); finally, a rise from the "I" level to the "P" level occurs (the maximum value of the fluorescence, F_M), due to congestion of electron traffic at the acceptor side of PSI.

Lotus japonicus (Leguminosae) has been broadly used as model plant to study many important physiological aspects during adaptation to salt stress, whose genome has been sequenced, providing numerous tools for genomic/genetic research (Handberg and Stougaard 1992; Sato and Tabata 2006). Several authors have compared the most widely employed genotypes of this species, Gifu B-129 and Miyakojima MG20 (MG20) using classic physiology and/or omic tools, regarding their tolerance and response to saline (Melchiorre et al. 2009; Sanchez et al. 2008, 2011, 2012) and alkaline stresses (Babuin et al. 2014; Campestre et al. 2016; Bordenave et al. 2017), showing that the first ecotype deploys a higher sensitivity level than the second ecotype to both stresses. In 2016, Campestre and collaborators registered a decline in PSII performance in plants of several *L. japonicus* ecotypes grown under alkaline condition. However, no study has been undertaken to compare Gifu B-129 and MG20 responses to combined saline–alkaline (S–A) stress, nor has any study been directed on those constituents of the PSII, which are substantially altered by saline, alkaline and S–A stresses in these ecotypes.

Our hypothesis are (1) PSII is vulnerable to salt stress in both ecotypes, (2) Gifu B-129 and MG20 deploy different responses to S–A stress, (3) the S–A stress causes higher damage levels than separated saline and alkaline stresses. To test this, we compared the impacts of three distinct classes of salt-induced stresses, alkaline, saline and S–A, on plant growth, net photosynthesis rate, stomatal conductance, Chl contents and specific Chl fluorescence parameters in the two model *L. japonicus* ecotypes.

Materials and methods

Plant material and growth conditions

L. japonicus seeds from MG20 and Gifu B-129 ecotypes were scarified with concentrated sulfuric acid (98%) 3 min, washed ten times with sterile distilled water and sown in Petri dishes containing water-agar (0.8%). Plates were incubated in a growth chamber at 30 °C in darkness until germination, 7 days after sown. Each resultant seedling was transferred to a 8 × 20-cm (diam × length) cylindrical pot containing washed sand mix (50% fine/50% coarse sand; pH 7.0; E.C. = 0.05 mS cm^{-1}) and irrigated with 0.5 × Hoagland's nutrient solution (Hoagland and Arnon 1950). Transferred plants were cultured in a growth chamber with a 16/8-h photoperiod at 24 °C/21 °C ± 2 °C (day/night) and 55/65 ± 5% relative humidity and 250 µmol photons m^{-2} s^{-1} light intensity provided by Grolux fluorescent lamps (F

40 W), until the end of all experiments. A drip irrigation system (9001 Digital Watering Timer Weekly Program, ELGO®, www.elgo.co.il; flow rate = 6.25 ml/h) was used according to Paz et al. (2012).

Experimental design and stress treatment

Experiments were performed according to a completely randomized design of one factor (stress) and four levels: control, saline, alkaline and S–A stresses.

The 0.5 × Hoagland solution was used as the nutrient source for all stressful and control conditions. The separate alkaline and saline conditions in a pot were created by adding, respectively, 10 mM $NaHCO_3$ and 100 mM NaCl to the nutrient solution. For the S–A treatment, 90 mM NaCl + 10 mM $NaHCO_3$ was added, thus obtaining a stress solution with the same Na^+-derived EC but a higher alkalinity than that of the saline stress treatment. Control treatment consisted of plants irrigated with 0.5 × Hoagland solution without NaCl or $NaHCO_3$. The pH and EC of irrigation solutions were monitored every 3 days with a combined pH meter/conductimeter (HI 255; Hanna Instruments, Padova, Italy) and maintained at 5.8/1.2, 5.8/11.0, 8.0/1.9 and 8.0/11.0 pH units/dS m^{-1}, for control, saline, alkaline and S–A conditions, respectively. In the case of alkaline treatment, 8-day-old seedlings received the final salt concentration: 10 mM $NaHCO_3$. To avoid any osmotic shock in the saline and S–A treatments, plants were first subjected to acclimation. For this, 8-day-old seedlings initially received 30 mM NaCl (saline), and 20 mM NaCl + 10 mM $NaHCO_3$ (S–A). Then NaCl concentration was stepwise increased during 1 week until reaching the final treatments concentrations. After acclimation, 15-day-old plants were grown under their respective treatments for further 20 days. Gas exchange parameters, Chl *a* fluorescence transients and chlorophyll contents were measured in 1-month-old plants, on intact, fully expanded leaves, which were basal to the internode immediately below the apical bud. Gas exchange and Chl *a* fluorescence transients were measured at midday. Plants were harvested at the age of 35 days, split into shoots and roots and kept for further determinations.

There were six plants per treatment for each measured parameter ($n = 6$), and the experiment was performed twice. Only most representative results are shown.

Evaluation of Gifu B-129 and MG20 tolerance

The tolerance of MG20 and Gifu B-129 genotypes to the different stress sources was evaluated on the base of the plant growth, in terms of total dry matter production. For this, roots and shoots were dried at 60 °C until constant weight.

Measurement of gas exchange parameters

Net photosynthesis rate (Pn), stomatal conductance (Gs), transpiration rate (E) and internal CO_2 (Ci) were measured under light saturation (1500 µmol photons m^{-2} s^{-1} illumination, LED light (peak wavelength: 625 nm), ambient carbon dioxide (400 ppm, average) at 24 °C, using a portable photosynthesis system (TPS-2 Portable Photosynthesis System, MA, USA). Data were collected at midday, 2 min to average steady state.

Measurement of Chl *a* fluorescence transient kinetic and OJIP parameters

Non-invasive Chl fluorescence fast-transient test (OJIP test) was conducted with a portable Chl fluorometer (PocketPEA v.1.1, Hansatech Instruments, Ltd., UK) at room temperature according to Babuin et al. (2014). Blade sections of intact leaves were covered with a leaf clip to adapt them to darkness for 20 min and then exposed for 3 s to 3500 µmol photons m^{-2} s^{-1} (637 nm peak wavelength) and Chl *a* fluorescence was recorded. The fluorescence data were processed by PEA plus software (Hansatech Instruments, U.K.) to obtain the OJIP parameters. Measurements were performed on six plants per treatment for each ecotype. A summary of OJIP parameters used in this study is shown in Table 1.

Chlorophyll *a* and *b* determination

Leaves were harvested and stored at − 80 °C until use. For pigment extraction, 40 mg of plant material grounded in liquid nitrogen was shaken in 100% acetone (4 °C, overnight). The extract was cold centrifuged and the supernatant removed. Measurements were made at wavelengths 663 nm (Chl *a*) and 647 nm (Chl *b*) in a spectrophotometer (Perkin Elmer Lambda 25 UV/VIS spectrometer), and pigment concentration was calculated according to Lichtenthaler (1987).

K^+, Na^+ and Cl^- determinations

The K^+ and Na^+ contents were extracted from shoots with 100 mM HCl and estimated by standard flame photometry according to Chen et al. (2001). Briefly, chloride was determined by a thiocyanate–Hg-based colorimetric reaction. For this, 12.5 mg of powdered dry plant material was extracted in 0.5 ml of a solution containing H_2O_2 (30%):concentrated HNO_3:isoamyl alcohol:H_2O at 1:1:0.08:7.9 (v/v), incubated at room temperature for 15 min, diluted to 5 ml with Milli-Q water, and vigorously agitated in a vortex. Then 1.5 ml of the extraction mixture was centrifuged (10,000 rpm, 5 min) and the supernatant transferred to another Eppendorf tube. The colorimetric reaction solution contained polyethylene glycol dodecyl ether–water (Brij 35®, 4%):mercuric thiocyanate

Table 1 Summary of parameters, formulae and their description using data extracted from chlorophyll *a* fluorescence (OJIP) transient (Strasser et al. 1999; Tsimilli-Michael and Strasser 2008)

	Description
Extracted parameters	
F_0	Minimum fluorescence at $t=0$, when all RC of PSII are open
F_M	Maximum fluorescence, when all RC of PSII are closed
Area	Total complementary area between the fluorescence induction curve and $F=F_M$
Derived parameters	
$F_V=F_{M-}F_0$	Maximal variable fluorescence
F_V/F_0	Proportional ratio to the activity of the water-splitting complex
$V_J=(F_{2\ ms-}F_0)/F_V$	Relative variable fluorescence at the J-step (2 ms)
$V_I=(F_{30\ ms-}F_0)/F_V$	Relative variable fluorescence at the I-step (30 ms)
$M_0=4\ (F_{300\ \mu s-}F_0)/F_V$	Approximated initial slope (in ms^{-1}) of the fluorescence transient
$S_s=V_J/M_0$	Normalized total complementary area corresponding only to the O–J phase
$S_m=\text{Area}/F_V$	Normalized total complementary area corresponding to the O–P phase or total electron carriers per RC
Quantum efficiencies	
F_V/F_M (or φP_0)	Maximum quantum efficiency of the PSII (primary photochemistry) at $t=0$
F_0/F_M (or φD_0)	Maximum quantum efficiency at $t=0$ for energy dissipation
$\psi E_0=1-V_J$	Quantum efficiency that an electron moves further than Q_A^-
Specific and phenomenological energy fluxes	
$\text{ABS/RC}=M_0\cdot(1/V_J)\cdot(1-\varphi P_0)$	Absorption flux (of antenna Chl) per RC
$\text{TR}_0/\text{RC}=M_0/V_J$	Trapped energy flux per RC at $t=0$
$\text{ET}_0/\text{RC}=M_0\cdot(1/V_J)\cdot(1-V_J)$	Electron transport flux per RC at $t=0$
$\text{DI}_0/\text{RC}=(\text{ABS/RC})-(\text{TR}_0/\text{RC})$	The flux of energy dissipated in processes other than trapping per active PSII
$\text{ABS/CS}_0=\text{Chl/CS}$	Absorption flux per cross section (CS) at $t=0$
RC densities and active Chl	
$\text{RC/CS}_0=\varphi P_0\cdot\text{ABS/CS}_0\cdot S_s$	Amount of RC per CS at $t=0$
$\text{RC/ABS}=\gamma\text{RC}/(1-\gamma\text{RC})$	Amount of RC per Chl
$\gamma\text{RC}=(1/(\text{ABS/RC}))/(1-(1/(\text{ABS/RC})))$	Probability that a PSII Chl molecule functions as RC
Performance index and its components	
$\gamma\text{RC}/(1-\gamma\text{RC})$	Structural component of PI_{ABS} (or EC)
$\varphi P_0/(1-\varphi P_0)$	Photochemical component of PI_{ABS} (or PC)
$\psi E_0/(1-\psi E_0)$	Biochemical component of PI_{ABS} (BC)
$\text{PI}_{\text{ABS}}=\text{EC}\cdot\text{PC}\cdot\text{BC}$	Performance index based on the equal absorption

(4.17 g/l methanol):$(NO_3)_3$Fe (202 g/l Milli-Q water plus 21 ml concentrated HNO_3):Milli-Q water at 0.05:15:15:70 (v/v). One milliliter of this reaction was added to 320 µl of the supernatant (control treatment). In the case of saline treatments, 50 µl of the supernatant was previously diluted to 320 µl with the extraction solution. Sample absorbance was determined at 450 nm with a spectrophotometer (Hitachi U-1100) and interpolated into a KCl calibration curve (0, 5, 10, 15, 20 ppm) to calculate Cl^- concentration.

Statistical analysis

The data of all parametric measurements were tested within each genotype through to one-way analysis of variance (ANOVA) and to multiple comparisons by Duncan's test. Statistical analyses were performed with the InfoStat package (Di Renzo et al. 2008).

Results

Impact of salinity, alkalinity and saline–alkaline treatments on plant growth and photosynthesis

Neutral, alkaline and mixed NaCl and $NaHCO_3$ salts significantly reduced total dry weight of Gifu B-129 and MG20 plants with respect to the control treatment (Fig. 1). The magnitude of the induced reductions due to salinity or mixed S–A stress tended to be higher in Gifu B-129 than in MG20 (respectively, 53% and 83% in the first, versus 34%

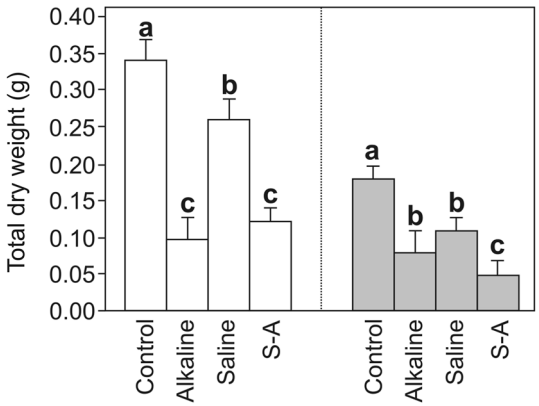

Fig. 1 Total dry weight of *L. japonicus* plants. Same letter within each ecotype means no statistical difference (Duncan's test, $P < 0.05$). Empty bars = MG20. Gray bars = Gifu B-129

and 61% in the second ecotype), and similar under alkalinity (Gifu B-129 = 61%; MG20 = 64%). Pn was reduced in both ecotypes by the mixed S–A stress, and by the alkaline stress in Gifu B-129 plants, whereas Gs and E were strongly reduced by the three types of stress in both ecotypes and Ci did not significantly vary (Table 2).

Effect of alkaline, saline and saline–alkaline treatments on Chl *a* fluorescence kinetics and behavior of PSII photosynthetic machine, determined by OJIP parameters

Chlorophyll fluorescence rise transients obtained from control leaves of both genotypes showed a typical OJIP shape (Fig. 2). The "spider plot" diagrams (Fig. 3) showed that the behavior of the different parameters characterizing PSII functioning varied according with the ecotype and the stress type. Overall, most significant variations with respect to the control situation were found in the S–A stress, those variations being more evident in Gifu B-129 than in MG20. Following paragraphs describing variations in fluorescence parameters were statistically supported by Duncan's test at $P < 0.05$.

No significant salt-induced changes in the OJIP curves were observed, except in Gifu B-129 plants treated with S–A stress, which showed a much lower fluorescence rise. Despite the fact that no salt-induced changes in F_0 and Fm were observed in Gifu B-129 (neither in MG20), some OJIP parameters derived from their relationship were affected by the S–A stress in this ecotype (Fig. 3a, b; Table 3): F_V/F_M (φP_0) and F_V/F_0 decreased (−5 and −10%, respectively), whereas F_0/F_M increased (20%).

Salt treatment also affected parameters normalized to F_V, although differently, according to the ecotype (Fig. 3a, b; Table 3). dV/dt_o, or M_0, reflects the accumulation rate of the active reaction center (RC) fraction that are closed, thus providing information about the acceptor side of PSII (Strasser et al. 1995, 2004; Strauss et al. 2006; Xia et al. 2004; Mehta et al. 2010a, b). M_0 was increased 68% by S–A stress in Gifu B-129 and reduced (21%) in MG20 treated with NaCl.

A rise in V_J suggests an increase of the proportions of closed RC and reduced Q_A at J step, whereas a rise in V_I indicates accumulations of reduced Q_A and plastoquinone, which cannot transfer electrons to the dark reactions (Pan et al. 2010). V_J was increased (40%) in Gifu B-129, and showed no change in MG20, whereas V_I showed mild increases in MG20 and Gifu B-129 under S–A stress, and in MG20 treated with $NaHCO_3$ alone. V_J and M_0 also defined the OJIP parameters $S_s = V_J/M_0$ and $Sm = Area/(F_M - F_0)$ that represent the normalized total complementary areas corresponding to the O–J phase and OP phase of the kinetic Chl fluorescence, respectively. S_s and S_m reflect the single-turnover Q_A reduction events and the multiple-turnover Q_A reduction events, respectively. S_s and S_m were reduced by S–A stress in Gifu B-129 (−25% and −39%, respectively). Conversely, MG20 increased the *S*s values under salinity and S–A stress (22 and 24%, respectively) and showed a slight fall of Sm (−8%) under S–A stress.

In the S–A treatment, the specific energy fluxes ABS/RC (or also, the absorption flux (of antenna chlorophylls) per RC, DI_0/RC and TR_0/RC showed contrasting

Table 2 Gas exchange parameters: net photosynthesis rate (P_n, μmol CO_2 m^{-2} s^{-1}), stomatal conductance (G_s, mmol H_2O m^{-2} s^{-1}), transpiration rate (E, mmol H_2O m^{-2} s^{-1}) and internal CO_2 (C_i, μmol mol^{-1}) in leaves of *L. japonicus* Gifu B-129 and MG-20 plants

Ecotype	Treatment	P_n	G_s	E	C_i
Gifu B-129	Control	1.8 ± 0.3a	39 ± 2.9a	0.58 ± 0.03a	412 ± 94ab
	Alkaline	0.6 ± 0.3b	25 ± 1.2b	0.33 ± 0.02b	359 ± 64ab
	Saline	1.5 ± 0.3a	17 ± 2.1c	0.26 ± 0.03c	331 ± 70b
	Mixed S–A	0.1 ± 0.2b	20 ± 1.2c	0.21 ± 0.02c	581 ± 85a
MG-20	Control	5.4 ± 0.4a	103 ± 6.4a	1.21 ± 0.05a	403 ± 35ab
	Alkaline	5.4 ± 0.6a	43 ± 4.3b	0.50 ± 0.04b	363 ± 32ab
	Saline	3.4 ± 0.7a	37 ± 2.7bc	0.43 ± 0.04bc	341 ± 33b
	Mixed S–A	0.1 ± 0.05b	30 ± 2.9c	0.35 ± 0.05c	455 ± 35a

Same letter within each ecotype means no statistical difference (Duncan's test, $P < 0.05$)

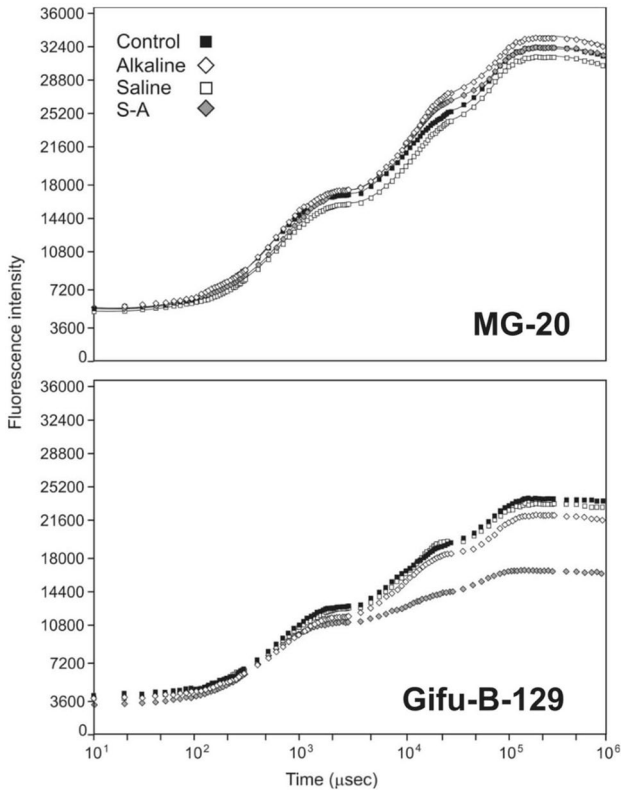

Fig. 2 Chlorophyll *a* fluorescence OJIP transient curves obtained from leaves MG20 and Gifu B-129

behaviors between genotypes since they decreased (15% average) in NaCl-treated MG20 plants, but increased (27% average) in Gifu B-129 ones (Fig. 3c, d; Table 3). On other hand, ET_0/RC was 15% average reduced by NaCl in both ecotypes, regardless alkalinity.

Under NaCl treatment, the density of RC or amount of RC per excited cross section (RC/CS_0) and the active Chl *a*ssociated with RC (γRC) of MG20 leaves were increased in a 20% and a notorious 130%, respectively, while these parameters showed no salt-induced change in Gifu B-129 (Fig. 3c, d; Table 3).

In Gifu B-129 plants, S–A stress induced 4%, 30% and 30% decreases of φP_0, and ψE_0 and φE_0, respectively (Fig. 3e, f; Table 3), whereas no changes in these parameters were registered in the remaining treatments.

PI_{ABS} is a multiparametric expression elaborated through independent components, all contributing to photosynthesis. PI_{ABS} was increased (29%) by NaCl as a sole stress source in MG20, whereas it was dramatically decreased by the S–A stress in Gifu B-129 (− 63%). In line, PI_{ABS} components behaved markedly different according to the ecotype and the type of salt (Fig. 3e, f; Table 3).

Effect of alkaline, saline and saline–alkaline treatments on the chlorophyll *a*nd ion contents

In Gifu B-129 plants, the S–A treatment led to decreased Chl *a* and total Chl contents, and reduced Chl *a*/*b* ratio, whereas no effect was observed on these parameters with the other two stresses (Fig. 4). In MG20, Chl b was reduced by the three types of salt stress, whereas Chl *a* was not affected. As result, total Chl content was reduced by the S–A stress, and no salt-induced change of the Chl *a*/*b* ratio was observed in this ecotype.

Higher shoot Na^+ and Cl^- levels were found in plants of both ecotypes when confronted with saline or S–A treatments, compared with respective controls (Supplementary Table 1). In contrast, a non-significant change was registered in these levels for plants treated with the alkaline salt alone. Regardless alkalinity, NaCl reduced K^+ contents and K^+/Na^+ ratios in plants of both ecotypes, whereas the alkaline salt added as a sole stress source affected these parameters only in Gifu B-129 plants.

Discussion

Salt stress impact on growth, gas exchange and ion contents

Although the main objective of this work was to gain insight into the salt-induced behavior of the *L. japonicus* photosynthetic apparatus, plant growth, gas exchange and ion accumulation were also analyzed to improve our knowledge on *L. japonicus* responses to the three stresses.

Our results from total biomass (Fig. 1) showed that the two ecotypes diverged in their sensitivity level to salinity, in agreement with earlier works (Sanchez et al. 2008, 2010), and that such divergence also applies to the S–A stress. In addition, we showed that both ecotypes were less tolerant to the last stress than to separate alkaline and saline stresses (in that order). A comparable result was previously reported by Paz et al. (2012) on plants of a different *Lotus* species, *L. tenuis*, subjected to the same three stress sources. Previous studies on other plant species have revealed that, when compared at the same concentration level, alkaline salts exert a more detrimental action on plant growth than neutral ones (Shi and Yin 1993; Tang and Turner 1999; Yang et al. 2008, 2009; Gong et al. 2013). It is worthy to note that the alkaline treatment here used had a much lower strength (10 mM of salt) than the saline one (100 mM of salt), what prevents us of confirming former statement. On the other hand, the S–A stress solution here employed had equal electrical conductivity to that of the saline treatment (neutral salt) and equal pH to that of the alkaline one. Therefore, the worse growth performance registered in the S–A treatment could

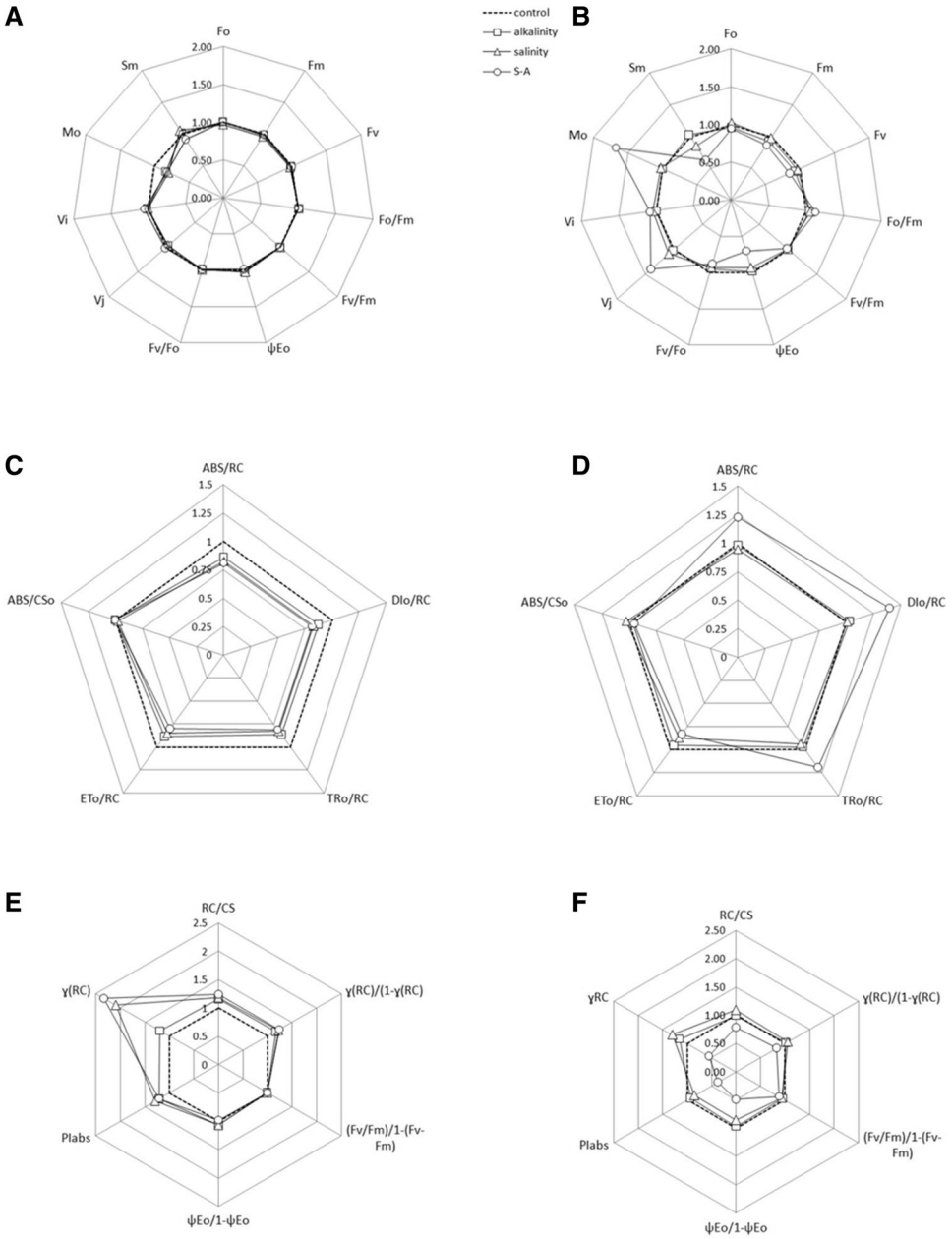

Fig. 3 Spider plots of the parameters measured and deduced from Chl *a* fluorescence OJIP transient curves in MG20 (**a**, **c**, **e**) and Gifu B-129 (**b**, **d**, **f**)

be a result of a possible additive effect of high saline strength and high pH.

In this work, some expected cause–effect relationships involving biomass and Gs parameters were not observed. Specifically, the negative effect of salt stress on plant biomass was not always accompanied by lower *P*n values, suggesting that factors such as a limited nutrient condition (Munns 2005; Tsai et al. 2004; Hong et al. 2009) or toxicity (Marschner 1995) may have intervened in such decreases. Indeed, this could be the case in our work: the reduced shoot K^+ content and K^+/Na^+ ratio, or the increased shoot Na^+ and Cl^- accumulation registered in some saline and alkaline treatments (Supplementary Table 1) to levels possibly toxic to diverse metabolic pathways, could have contributed to the reduction of the total biomass in those treatments. In fact, the higher ability of MG20, compared to Gifu B-129 to prevent Na^+ reaching the shoot was the physiological parameter better explaining the more satisfactory response to salt stress of the first ecotype, in terms of plant biomass. Likewise, significant stress-induced stomatal closures were registered in both genotypes, in the absence of photosynthetic performance variation. The last phenomenon has been previously reported by other authors (Munns and Tester 2008; James et al. 2002) and may be explained through salt-induced changes in leaf anatomy leading to the improvement in CO_2 diffusion (Acosta-Motos et al. 2015a,

Table 3 Significant variations (%) observed in the different OJIP parameters in MG20 and Gifu B-129 plants under the three stressful conditions in comparison with the control (Duncan's test, $P<0.05$)

Parameter	Description	MG20			Gifu B-129		
		Alkaline	Saline	S–A	Alkaline	Saline	S–A
Extracted and derived parameters							
F_0	Minimum fluorescence at $t=0$, when all RC of PSII are open	–	–	–	–	–	–
F_M	Maximum fluorescence, when all RC of PSII are closed	–	–	–	–	–	–
F_V	Maximal variable fluorescence (F_M–F_0)	–	–	–	–	–	–
F_V/F_0	Proportional ratio to the activity of the water-splitting complex	–	–	–	–	–	−10
V_J	Accumulations of Q_A^-	–	–	–	–	–	40
V_I	Accumulations of Q_A^- and reduced PQ	5	–	5	–	–	9
M_0	Accumulation rate of closed RC	–	−21	−21	–	–	68
S_s	Reflects the single-turnover Q_A reduction events		22	24			−21
S_m	Reflects the multiple-turnover Q_A reduction events or total electron carriers per RC	–	–	–	–	–	−39
Quantum efficiencies							
φP_0	Efficiency of PSII to reduce Q_A	–	–	–	–	–	−5
φD_0	Efficiency for energy dissipation	–	–	–	–	–	20
ψE_0	Efficiency to move an electron further than Q_A^-	–	–	–	–	–	−30
Specific energy and phenomenological fluxes							
ABS/RC	Absorption flux (of antenna Chl) per RC	–	−15	−19	–	–	23
TR_0/RC	Trapped energy flux per RC at $t=0$	–	−16	−21	–	–	19
ET_0/RC	Electron transport flux per RC at $t=0$	–	−10	−19	–	−13	−17
DI_0/RC	The flux of energy dissipated in processes other than trapping per active PSII	–	−13	−13	–	–	36
ABS/CS_0	Absorption flux per cross section (CS) at $t=0$	–	–	–	–	–	–
RC densities, active Chl in RC, performance indices and components							
RC/CS_0	Amount of RC per CS at $t=0$	–	18	24	–	–	–
γRC	Probability that a PSII Chl molecule functions as RC	–	121	135	–	–	–
$\gamma RC/(1-\gamma RC)$	Structural component of PI_{ABS}	–	17	23	–	–	−17
$\varphi P_0/(1-\varphi P_0)$	Photochemical component of PI_{ABS}	–	–	–	–	–	−12
$\psi E_0/(1-\psi E_0)$	Biochemical component of PI_{ABS}	–	–	–	–	–	−50
PI_{ABS}	Performance index based on the equal absorption	–	29	–	–	–	−63

Dash line means no significant differences, compared with the control treatment

b; Gómez-Bellot et al. 2015). In this regard, it is worth to mention that alkaline and S–A salts caused a replacement of palisade by spongy parenchyma in leaves of *L. tenuis* (Paz et al. 2014). Further anatomical studies performed on *L. japonicus* ecotypes MG20 and Gifu B-129, testing the hypothesis of a salt-induced reorganization of leaf mesophyll would be valuable for a better understanding of present gas exchange results.

Salt stress impact on PSII photosynthetic performance

Data pertaining to the Chl fluorescence analysis showed that the most significant effects induced by salt addition concerned Gifu B-129 plants treated with combined neutral–alkaline salts, and MG20 plants treated with NaCl. The two photosynthesis-related indexes, φP_0 and PI_{ABS}, were found to be notably altered by diverse environmental constraints in several plant species (Pietrini et al. 2005; Gazquez et al. 2015, 2018). As φP_0 may provide clues of photoinhibition occurrence (Yamane et al. 2008; Goh et al. 2012), our data showing no significant salt-induced variation in this parameter (or a −4% decrease in Gifu under S–A) suggest the absence of photoinhibition events due to salt treatment. The φP_0 also reflects the PSII capacity to reduce the primary acceptor Q_A (Calatayud and Barreno 2001). The PI_{ABS} is regulated by the three main functional steps of photosynthetic activity by the PSII, which are absorption of light energy (ABS), trapping of excitation energy (TR) and conversion of excitation energy (ET; Strasser et al. 2000). The fact that both parameters were reduced by combined NaCl and $NaHCO_3$ salts in Gifu B-129 plants (Fig. 3), but not in MG20, supports the notion extracted from biomass data of a higher tolerance to the S–A stress in the last ecotype,

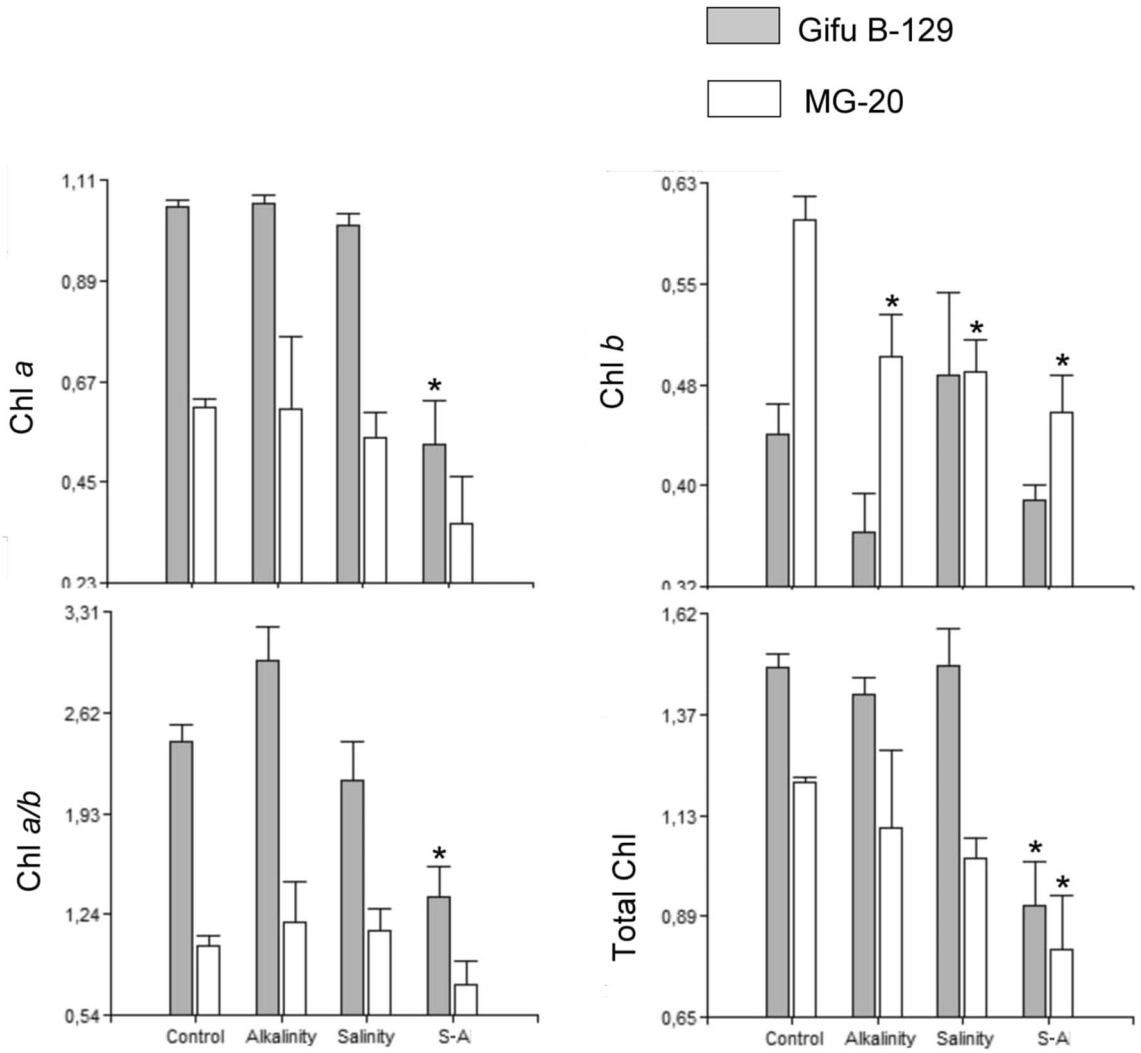

Fig. 4 Contents of Chl *a*, b, Chl *a*/b ratio and total Chl content in apical leaves of Gifu B-129 and MG20 plants. Asterisks mean statistical difference from control at $P < 0.05$, according to Duncan's Test

compared with Gifu B-129. Interestingly, NaCl alone increased PI_{ABS} in MG20 plants, indicating an improvement of the PSII functioning in these plants. However, last result was not reflected by P_n values. This lack of parallelism between net photosynthesis and the mentioned indices may be explained by the electron flux being not used in carbon metabolism, but re-routed to other biochemical pathways such as Mehler reaction, or photorespiration (which may sum 36% of photosynthetic electrons dissipated, e.g., in tomato under water stress; Haupt-Herting and Fock 2002).

Salt stress-induced modifications of the photosynthetic apparatus structures

RC/ABS and RC/CS are measures of the density of RC per ABS and cross section or CS, respectively. The most commonly observed RC response to salinity in glycophytes is their reduction, (e.g., *Scenedesmus obliquus*, Demetriou et al. 2007; *Cucumis melo*, Xiang et al. 2016; *Triticum sp*, Mehta et al. 2010a, b; *Wolffia arrhiza,* Wang et al. 2011 and *Solanum lycopersicum,* Zushi and Matsuzoe 2017). In this study, the RC pool size was another parameter differently altered by salt stress according to the ecotype. RC reduction was registered in Gifu B-129 plants exposed to combined NaCl and $NaHCO_3$ salts, confirming the glycophytic *L. japonicus* status (Sanchez et al. 2008, 2011). In contrast, both RC densities (per both cross section and absorption energy flux) increased in NaCl-treated MG20 plants, in line with higher values of ɣRC, registered in this ecotype. Having in mind that salt-treated plants of the halophyte *Artemisia anethifolia* presented higher RC/CS than corresponding controls (Wen et al. 2005), former result could be interpreted as an adaptation, through improvement of RC stability, of the photosystem machinery to NaCl in

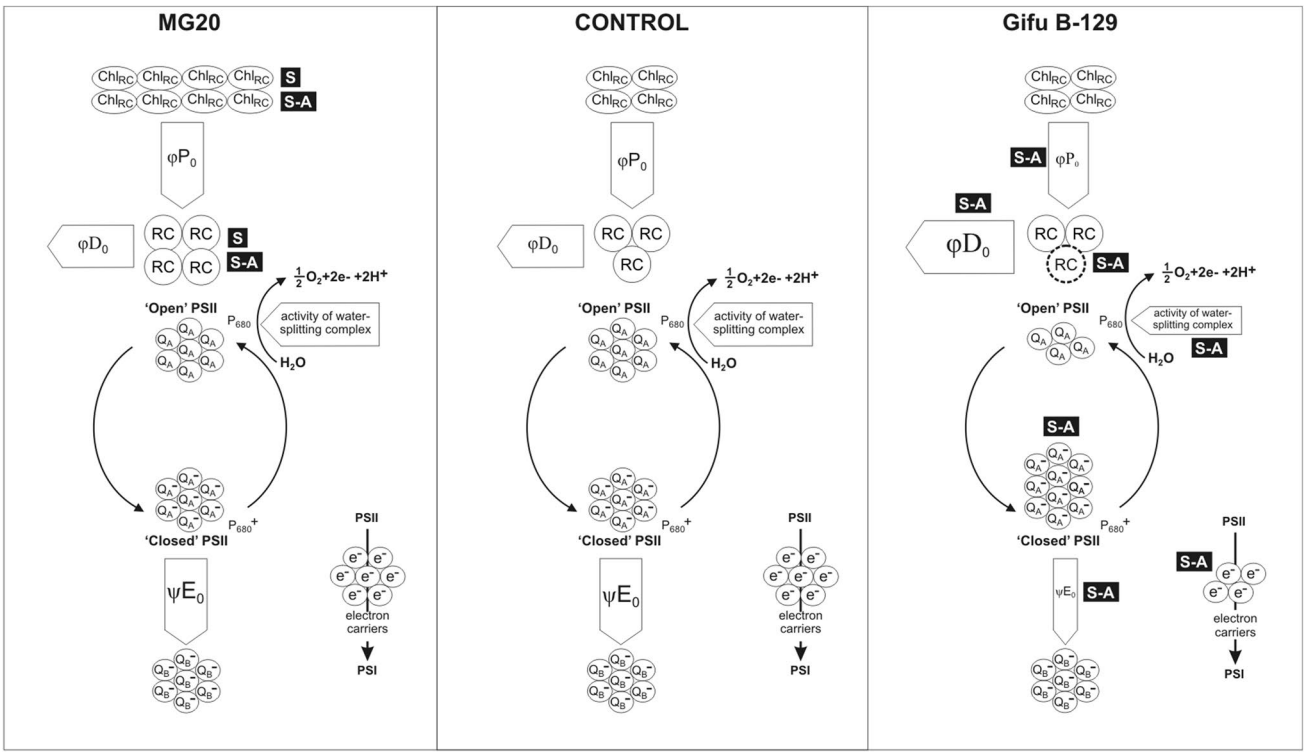

Fig. 5 Schematic representation of OJIP test results. Central block represents a control condition for both ecotypes. Right and left blocks depict the sets of salt-induced events revealed by Chl fluorescence data in MG20 and Gifu B-129. Black boxes with A, S or S–A mean alkaline, saline or S–A treatments, respectively. *RC* active reaction center, RC with dashed line means "non-RC"; Chl_{RC} active Chl in RC, Q_A and Q_A^- quinone A oxidized and reduced, respectively. Smaller and bigger arrows and letters with respect to the central block mean negative and positive changes regarding quantum efficiencies and the activity of the water-splitting complex, compared with the untreated control

this ecotype. Interestingly, the MG20 ecotype was considered as a moderate halophyte by Melchiorre and collaborators (2009) when confronted with 50 mM NaCl. Thus, the opposite S–A-induced responses observed in the RC/ABS between genotypes, an increase in MG20 and a decrease in Gifu B-129, could have also contributed with the contrasting behavior of PI_{ABS} in these ecotypes.

Variations in the effective antenna size of PSII may be inferred from changes in ABS/RC, chlorophyll content and Chl *a*/*b* ratio. These parameters varied concomitantly in Gifu B-129 plants under the mixed S–A treatment, supporting the notion that mixed NaCl and $NaHCO_3$ salts induced a higher effective antenna size in this last ecotype, with preferential loss of reactions center complexes (DI0/RC, Table 3; Figs. 3, 4). In parallel, the chlorophyll contents and chl a/b data support specific loss of LHC in MG-20.

Salt effects on electron transport chain and carriers

Changes in several obtained and calculated parameters support the notion that, in Gifu B-129 plants confronting mixed (neutral and alkaline) salts, photoinhibition took place on both sides of PSII (acceptor and donor). On the one hand, the reduction in Fv/F_0 reflects a decrease in the water-splitting complex activity, at the donor PSII site (Schreiber et al. 1995; Sayed 1998; Kalaji et al. 2011). Also, the decrease of *Ss* values in Gifu B-129 under S–A stress indicated a detriment of the processes associated with the primary photochemistry. Interestingly, higher *Ss* values in MG20 under saline and S–A stresses would indicate an improvement of the primary photochemistry. On the other hand, the decrease in ψE_0 and the rise in V_I, V_J and M_0 in Gifu B-129 plants treated with combined NaCl and $NaHCO_3$ salts conform to the idea of a slowdown of electron transfer from Q_A to the secondary acceptor Q_B, on the acceptor PSII side. Also, the decrease in *Sm* registered in Gifu B-129 plants under S–A stress suggests a decline in the pool of electron carriers between PSII and PSI, as *Sm* reflects the total electron carriers per RC (Jiang et al. 2008). Last results point to a reduction of the total electron acceptor capacity of S–A-treated Gifu B-129 leaves. Besides (unlike MG20), Gifu B-129 plants under S–A treatment presented increased TR_0/RC although there was no significant change in the RC level. According to Wen et al. (2005), last situation indicates a lower Q_A re-oxidation. In fact, our data showing a reduction in the electron transport per reaction center (ET_0/RC)

in these plants are in line with the last phenomenon, and support the decreased ψE_0, and the increased DI_0/RC (non-photochemical quenching of energy) registered. Indeed, this scenery of electron transport blockage, in addition to a higher effective antenna size as it was pictured above for Gifu B-129, explains the higher energy dissipation of the excess excitation energy trapped in the non-RC (DI_0/RC, Fig. 3d, Table 3). A rise in non-photochemical quenching may be the outcome of changes in either photoinhibition or protective high-energy-state quenching. As we stated above, our results from φP_0 suggested the absence of photoinhibition events due to salt treatment. In tomato, increasing non-photochemical quenching, associated with lower φP_0, was suggested to intervene in excess energy dissipation to keep photosynthetic apparatus from being dismantled (Gong et al. 2013). Energy dissipation prevents the reduction of Q_A to Q_A^- and, therefore, it does not contribute to the variable fluorescence (see Strasser and Strasser 1995; Strasser et al. 2000; Krüger et al. 1997; Appenroth et al. 2001; Jafarinia and Shariati 2012). That is why the OJIP curves obtained from Gifu B-129 plants treated with combined NaCl and $NaHCO_3$ salts presented lower fluorescence levels than those from control plants (Fig. 2). Taken as a whole, these results explain the observed PI_{ABS} and φP_0 decreases in the Gifu B-129 ecotype.

Conclusions

Figure 5 summarizes the effects of different stresses on the photosynthetic apparatus of both genotypes, explained on the base of their energy fluxes, quantum yields and efficiencies, and pools of each photosynthetic machine component. Our results allow us to accept the proposed hypothesis. Here we conclude that NaCl-derived stress sources affect the photochemical events in PSII in both ecotypes, being this effect more evident under higher pH condition, whereas alkalinity per se has a mild or no effect on these events. Our study also allowed us to determine quantitative and qualitative differences between both ecotypes regarding Chl *a* fluorescence response to salt stresses. The S–A treatment induced a more severe effect on Gifu B-129, compared with MG20, particularly on those parameters related to the functioning of a section spanning the donor (water-splitting complex) and the first acceptor (Q_A) sides of the electron transport chain. In contrast, NaCl improved primary photochemistry in MG20, although the step between Q_B and PSI was functionally compromised in this ecotype. The fact that some components or sequential steps of the PSII photosynthetic activity in Gifu B-129 and MG20 had diverged during their salt-induced responses indicates that both model ecotypes would not be equivalents for performing experiments addressing more specific hypothesis on physicochemical or structural aspects of the *L. japonicus* photosynthetic machinery. Therefore, we consider the information here obtained is useful and should be taken into account in future research on structural and biochemical aspects of the photosynthetic apparatus, aimed at elucidating the mechanisms that make possible the tolerance to these stressful conditions.

Author contribution statement ABM: conceptualization; RR, CDB and MPC: methodology; ABM and AAR: formal analysis; SJM and OAR: funding acquisition; ABM: writing original draft; ABM, AAR and CDB: writing review and editing.

Acknowledgements This work was supported by Grants from the Agencia Nacional de promoción Científica y Tecnológica/FONCyT PICTs 2034 and 1611, and the Consejo Nacional de Investigaciones Científicas y Técnicas (CONICET, Argentina).

References

Acosta-Motos JR, Diaz-Vivancos P, Alvarez S, Fernández-García N, Sánchez-Blanco MJ, Hernández JA (2015a) NaCl-induced physiological and biochemical adaptative mechanisms in the ornamental *Myrtus communis* L plants. J Plant Physiol 183:41–51

Acosta-Motos JR, Diaz-Vivancos P, Álvarez S, Fernández-García N, Sanchez-Blanco MJ, Hernández JA (2015b) Physiological and biochemical mechanisms of the ornamental *Eugenia myrtifolia* L plants for coping with NaCl stress and recovery. Planta 242:829–846

Appenroth KJ, Stöckel J, Srivastava A, Strasser RJ (2001) Multiple effects of chromate on the photosynthetic apparatus of *Spirodela polyrhiza* as probed by OJIP chlorophyll *a* fluorescence measurement. Environ Pollut 115:49–64

Ashraf MHPJC, Harris PJC (2013) Photosynthesis under stressful environments: an overview. Photosynthetica 51:163–190

Babuin MF, Campestre MP, Rocco R, Bordenave CD, Escaray FJ, Antonelli C, Calzadilla P (2014) Response to long-term $NaHCO_3$-derived alkalinity in model *Lotus japonicus* ecotypes Gifu B-129 and miyakojima MG-20: transcriptomic profiling and physiological characterization. PLoS ONE 9:e97106

Bordenave CD, Rocco R, Babuin MF, Campestre MP, Escaray FJ, Gárriz A, Antonelli C (2017) Characterization of the primary metabolome during the long-term response to $NaHCO_3$-derived alkalinity in *Lotus japonicus* ecotypes Gifu B-129 and Miyakojima MG-20. Acta Physiol Plant 39:76

Calatayud A, Barreno E (2001) Chlorophyll *a* fluorescence antioxidant enzymes and lipid peroxidation in tomato in response to ozone and benomyl. Environ Pollut 115:283–289

Campestre MP, Antonelli C, Calzadilla PI, Maiale SJ, Rodríguez AA, Ruiz OA (2016) The alkaline tolerance in *Lotus japonicus* is associated with mechanisms of iron acquisition and modification of the architectural pattern of the root. J Plant Physiol 206:40–48

Chaves MM, Flexas J, Pinheiro C (2009) Photosynthesis under drought and salt stress: regulation mechanisms from whole plant to cell. Ann Bot-London 103:551–560

Chen S, Li J, Wang S, Hüttermann A, Altman A (2001) Salt nutrient uptake and transport and ABA of *Populus euphratica* a hybrid in response to increasing soil NaCl. Trees 15:186–194

Clark RB (1982) Iron deficiency in plants grown in the Great Plains of the US. J Plant Nut 5:251–268

Clark RB, Yusuf Y, Ross WM, Maranville JW (1982) Screening for sorghum genotypic differences to iron deficiency. J Plant Nut 5:587–604

Demetriou G, Neonaki C, Navakoudis E, Kotzabasis K (2007) Salt stress impact on the molecular structure and function of the photosynthetic apparatus—the protective role of polyamines. BBA-Bioenergetics 1767:272–280

Di Renzo JA, Casanoves F, Balzarini MG, González L, Tablada M, Robledo CW (2008) Infostat versión Grupo InfoStat FCA. Universidad Nacional de Córdoba, Argentina

Duarte B, Santos D, Marques JC, Caçador I (2013) Ecophysiological adaptations of two halophytes to salt stress: photosynthesis PS II photochemistry and anti-oxidant feedback–implications for resilience in climate change. Plant Physiol Bioch 67:178–188

Gazquez A, Maiale SJ, Rachoski MM, Vidal A, Ruiz OA, Menéndez AB, Rodríguez AA (2015) Physiological response of multiple contrasting rice (*Oryza sativa* L) cultivars to suboptimal temperatures. J Agron Crop Sci 201:117–127

Gazquez A, Vilas JM, Lerner JEC, Maiale SJ, Calzadilla PI, Menéndez AB, Rodríguez AA (2018) Rice tolerance to suboptimal low temperatures relies on the maintenance of the photosynthetic capacity. Plant Physiol Bioch 127:537–552

Goh CH, Ko SM, Koh S, Kim YJ, Bae HJ (2012) Photosynthesis and environments: photoinhibition and repair mechanisms in plants. J Plant Biol 55:93–101

Goltsev VN, Kalaji HM, Paunov M, Bąba W, Horaczek T, Mojski J, Kociel H (2016) Variable chlorophyll fluorescence and its use for assessing physiological condition of plant photosynthetic apparatus. Russ J Plant Physiol 63:869–893

Gómez-Bellot MJ, Nortes PA, Ortuño MF, Romero C, Fernandez-Garcia N, Sánchez-Blanco MJ (2015) Influence of arbuscular mycorrhizal fungi and treated wastewater on water relations and leaf structure alterations of *viburnum tinus* L plants during both saline and recovery periods. J Plant Physiol 188:96–105

Gong B, Wena D, VandenLangenberg K, Wei M, Yanga F, Shi Q, Wanga X (2013) Comparative effects of NaCl and $NaHCO_3$ stress on photosynthetic parameters, nutrient metabolism, and the antioxidant system in tomato leaves. Sci Hort 157:1–12

Handberg K, Stougaard J (1992) *Lotus japonicus* an autogamous diploid legume species for classical and molecular genetics. Plant J 2:487–496

Haupt-Herting S, Fock HP (2002) Oxygen exchange in relation to carbon assimilation in water-stressed leaves during photosynthesis. Ann Bot-London 89:851–859

Hoagland DR, Arnon DI (1950) The water-culture method for growing plants without soil. In: Circular California agricultural experiment station, vol 347, 2nd edn

Hong CY, Chao YY, Yang MY, Cho SC, Kao CH (2009) Na^+ but not Cl^- or osmotic stress is involved in NaCl-induced expression of glutathione reductase in roots of rice seedlings. J Plant Physiol 166:1598–1606

Jafarinia M, Shariati M (2012) Effects of salt stress on photosystem II of canola plant (*Barassica napus* L) probing by chlorophyll *a* fluorescence measurements. Iran J Sci Technol 36:71–76

James RA, Rivelli AR, Munns R, von Caemmerer S (2002) Factors affecting CO_2 assimilation leaf injury and growth in salt-stressed durum wheat. Funct Plant Biol 29:1393–1403

Jia XM, Wang H, Svetla S, Zhu Y-F, Hu Y, Chen L, Zhao T, Wang YX (2019) Comparative physiological responses and adaptive strategies of apple *Malus halliana* to salt, alkali and saline-alkali stress. Sci Hortic 245:154–162

Jiang HX, Chen LS, Zheng JG, Han S, Tang N, Smith BR (2008) Aluminum-induced effects on photosystem II photochemistry in citrus leaves assessed by the chlorophyll *a* fluorescence transient. Tree Physiol 28:1863–1871

Kalaji HM, Bosa K, Kościelniak J, Żuk-Gołaszewska K (2011) Effects of salt stress on photosystem II efficiency and CO_2 assimilation of two syrian barley landraces. Environ Exp Bot 73:64–72

Krüger GH, Tsimilli-Michael M, Strasser RJ (1997) Light stress provokes plastic and elastic modifications in structure and function of photosystem II in camellia leaves. Physiol Plant 101:265–277

Kukavica B, Morina F, Janjić N, Boroja M, Jovanović L, Veljović-Jovanović S (2013) Effects of mixed saline and alkaline stress on the morphology and anatomy of *Pisum sativum* L: the role of peroxidase and ascorbate oxidase in growth regulation. Arch Biol Sci 65:265–278

Kumar A, Kumar A, Kumar P, Lata C, Kumar S (2018) Effect of individual and interactive alkalinity and salinity on physiological, biochemical and nutritional traits of marvel grass. Ind J Exp Biol 56:573–581

Kyle DJ, Osmond CB, Arntzen CJ (eds) (1987) Photoinhibition, topics in photosynthesis, vol 9. Elsevier, Amsterdam, pp 289–307

Läuchli A, Lüttge U (2002) Salinity: environment-plants-molecules. Kluwer Academic Publishers, Dordrecht, pp 229–248

Li R, Shi F, Fukuda K (2010) Interactive effects of various salt and alkali stresses on growth organic solutes and cation accumulation in a halophyte *Spartina alterniflora* (Poaceae). Environ Exp Bot 68:66–74

Li Z, Cong R, Yang Q, Zhou J (2017) Effects of saline-alkali stress on growth and osmotic adjustment substances in willow seedlings. Acta Ecol Sin 37:8511–8517

Lichtenthaler FW (1987) Karl Freudenberg, Burckhardt Helferich, Hermann OL Fischer A centennial tribute. Carbohyd Res 164:1–22

Marschner H (1995) Mineral nutrition of higher plants, 2nd edn. Academic Press, London

Mathur S, Mehta P, Jajoo A (2013) Effects of dual stress (high salt and high temperature) on the photochemical efficiency of wheat leaves (*Triticum aestivum*). Physiol Mol Biol Plant 19:179–188

Mehta P, Jajoo A, Mathur S, Bharti S (2010a) Chlorophyll *a* fluorescence study revealing effects of high salt stress on photosystem II in wheat leaves. Plant Physiol Biochem 48:16–20

Mehta P, Allakhverdiev SI, Jajoo A (2010b) Characterization of photosystem II heterogeneity in response to high salt stress in wheat leaves (*Triticum aestivum*). Photosynth Res 105:249–255

Melchiorre M, Quero GE, Parola R, Racca R, Trippi VS, Lascano R (2009) Physiological characterization of four model lotus diploid genotypes: *L. japonicus* (MG20 and Gifu) *L. filicaulis* and *L. burttii* under salt stress. Plant Sci 177:618–628

Munns R (2002) Comparative physiology of salt and water stress. Plant Cell Environ 25:239–250

Munns R (2005) Genes and salt tolerance: bringing them together. New Phytol 167:645–663

Munns R, Tester M (2008) Mechanisms of salinity tolerance. Annu Rev Plant Biol 59:651–681

Pan X, Zhang D, Chen X, Li L, Mu G, Li L, Song W (2010) Sb uptake and photosynthesis of *Zea mays* growing in soil watered with Sb mine drainage: an OJIP chlorophyll fluorescence study. Pol J Environ Stud 19:981

Papageorgiou G (1975) Chlorophyll fluorescence: an intrinsic probe of photosynthesis. In: Govindjee (ed) Bioenergetics of photosynthesis. Academic Press, pp 319–371

Parida AK, Das AB (2005) Salt tolerance and salinity effects on plants: a review. Ecotoxi Environ Saf 60:324–349

Paz RC, Rocco RA, Reinoso H, Menéndez AB, Pieckenstain FL, Ruiz OA (2012) Comparative study of alkaline saline and mixed saline–alkaline stresses with regard to their effects on growth

nutrient accumulation and root morphology of *Lotus tenuis*. J Plant Growth Regul 31:448–459
Paz RC, Reinoso H, Espasandin FD, González Antivilo FA, Sansberro PA, Rocco RA, Ruiz OA (2014) Akaline saline and mixed saline–alkaline stresses induce physiological and morpho-anatomical changes in *Lotus tenuis* shoots. Plant Biol 16:1042–1049
Pietrini F, Chaudhuri D, Thapliyal AP, Massacci A (2005) Analysis of chlorophyll fluorescence transients in mandarin leaves during a photo-oxidative cold shock and recovery. Agr Ecosyst Environ 106:189–198
Sanchez DH, Lippold F, Redestig H, Hannah MA, Erban A, Krämer U, Kopka J (2008) Integrative functional genomics of salt acclimatization in the model legume *Lotus japonicus*. Plant J 53:973–987
Sanchez DH, Szymanski J, Erban A, Udvardi MK, Kopka J (2010) Mining for robust transcriptional and metabolic responses to long-term salt stress: a case study on the model legume *Lotus japonicus*. Plant Cell Environ 33:468–480
Sanchez DH, Pieckenstain FL, Szymanski J, Erban A, Bromke M, Hannah MA, Kraemer U (2011) Comparative functional genomics of salt stress in related model and cultivated plants identifies and overcomes limitations to translational genomics. PLoS One 6:e17094
Sanchez DH, Schwabe F, Erban A, Udvardi MK, Kopka J (2012) Comparative metabolomics of drought acclimation in model and forage legumes. Plant Cell Environ 35:136–149
Sato S, Tabata S (2006) *Lotus japonicus* as a platform for legume research. Curr Opin Plant Biol 9:128–132
Sayed OH (1998) Analysis of photosynthetic responses and adaptation to nitrogen starvation in Chlorella using in vivo chlorophyll fluorescence. Photosynthetica 35:611–619
Schreiber UBWN, Bilger W, Neubauer C (1995) Chlorophyll fluorescence as a nonintrusive indicator for rapid assessment of in vivo photosynthesis. Ecophysiology of photosynthesis. Springer, Berlin, Heidelberg, pp 49–70
Shi D, Sheng Y (2005a) Effect of various salt–alkaline mixed stress conditions on sunflower seedlings and analysis of their stress factors. Environ Exp Bot 54:8–21
Shi D, Wang D (2005b) Effects of various salt-alkaline mixed stresses on *Aneurolepidium chinense* (Trin) Kitag. Plant Soil 271:15–26
Shi D, Yin L (1993) Difference between salt (NaCl) and alkaline (Na_2CO_3) stresses on *Puccinellia tenuiflora* (Griseb.) Scribn et Merr Plants. Acta Bot Sin 3:144–149
Strasser RJ, Govindjee (1992) On the O-J-I-P fluorescence transients in leaves and Dl mutants of Chlamydomonas reinhardtii. In: Murata N (ed) Research in photosynthesis, vol II, pp 29–32. Kluwer Academic, Dordrecht
Strasser BJ, Strasser RJ (1995) Measuring fast fluorescence transients to address environmental questions: the JIP-Test. In: Mathis P (ed) Photosynthesis: from light to biosphere. KAP Press, Dordrecht, pp 977–980. https://doi.org/10.1007/978-94-009-0173-5_1142
Strasser RJ, Srivastava A, Govindjee G (1995) Polyphasic chlorophyll *a* fluorescence transient in plants and cyanobacteria. Photochem Photobiol 61:32–42
Strasser RJ, Srivastava A, Tsimilli-Michael M (1999) Screening the vitality and photosynthetic activity of plants by fluorescence transient. In: Behl RK, Punia MS, Lather BPS (eds) Crop improvement for food security. SSARM, Hisar, pp 72–115
Strasser RJ, Srivastava A, Tsimilli-Michael M (2000) The fluorescence transient as a tool to characterise and screen photosynthetic samples. In: Yunus M, Pathre U, Mohanty P (eds) Probing photosynthesis: mechanisms, regulation and adaptation. Taylor and Francis, London, New York, pp 445–483
Strasser RJ, Tsimilli-Michael M, Srivastava A (2004) Analysis of the chlorophyll *a* fluorescence transient. Chlorophyll *a* fluorescence. Springer, Dordrecht, pp 321–362
Strauss AJ, Krüger GHJ, Strasser RJ, Van Heerden PDR (2006) Ranking of dark chilling tolerance in soybean genotypes probed by the chlorophyll *a* fluorescence transient OJIP. Environ Exp Bot 56:147–157
Tang C, Turner NC (1999) The influence of alkalinity and water stress on the stomatal conductance photosynthetic rate and growth of *Lupinus angustifolius* L and *Lupinus pilosus*. Aust J Exp Agr 39:457–464
Tester M, Davenport R (2003) Na^+ tolerance and Na^+ transport in higher plants. Ann Bot-London 91:503–527
Tsai YC, Hong CY, Liu LF, Kao CH (2004) Relative importance of Na^+ and Cl^- in $NaCl^-$ induced antioxidant systems in roots of rice seedlings. Physiol Plant 122:86–94
Tsimilli-Michael M, Strasser RJ (2008) In vivo assessment of plants' vitality: applications in detecting and evaluating the impact of mycorrhization on host plants. In: Varma A (ed) Mycorrhiza. Springer, Berlin, Heidelberg, pp 679–703
Vu TS, Zhang D, Xiao W, Chi C, Xing Y (2015) Mechanisms of combined effects of salt and alkaline stresses on seed germination and seedlings of *Melilotus officinales* (Fabaceae) in Northeast of China. Pak J Bot 47:1603–1611
Wang G, Chen L, Hao Z, Li X, Liu Y (2011) Effects of salinity stress on the photosynthesis of *Wolffia arrhiza* as probed by the OJIP test. Fresenius Environ Bull 20:432–438
Wen X, Qiu N, Lu Q, Lu C (2005) Enhanced thermotolerance of photosystem II in salt-adapted plants of the halophyte *Artemisia anethifolia*. Planta 220:486–497
Xia J, Li Y, Zou D (2004) Effects of salinity stress on PSII in *Ulva lactuca* as probed by chlorophyll fluorescence measurements. Aquat Bot 80:129–137
Xiang L, Hu L, Xu W, Zhen A, Zhang L, Hu X (2016) Exogenous γ-aminobutyric acid improves the structure and function of photosystem II in muskmelon seedlings exposed to salinity-alkalinity stress. PLoS One 11:e0164847
Yamane K, Kawasaki M, Taniguchi M, Miyake H (2008) Correlation between chloroplast ultrastructure and chlorophyll fluorescence characteristics in the leaves of rice (*Oryza sativa* L.) grown under salinity. Plant Prod Sci 11:139–145
Yang C, Chong J, Li C, Kim C, Shi D, Wang D (2007) Osmotic adjustment and ion balance traits of an alkali resistant halophyte *Kochia sieversiana* during adaptation to salt and alkali conditions. Plant Soil 294:263–276
Yang CW, Jianaer A, Li CY, Shi DC, Wang DL (2008) Comparison of the effects of salt-stress and alkali-stress on photosynthesis and energy storage of an alkali-resistant halophyte *Chloris virgata*. Photosynthetica 46:273–278
Yang CW, Xu HH, Wang LL, Liu J, Shi DC, Wang DL (2009) Comparative effects of salt-stress and alkali-stress on the growth, photosynthesis, solute accumulation, and ion balance of barley plants. Photosynthetica 47:79–86
Yeo A (1998) Molecular biology of salt tolerance in the context of whole-plant physiology. J Exp Bot 49(323):915–929
Zushi K, Matsuzoe N (2017) Using of chlorophyll *a* fluorescence OJIP transients for sensing salt stress in the leaves and fruits of tomato. Sci Hort 219:216–221